Long-term kinetics of DNA interacting with polycations

Cui Zheng [a],[1], Lin Niu [a],[1], Wei Pan [a], Jihan Zhou [a], Hua Lv [b], Jianjun Cheng [b], Dehai Liang [a],*

[a] Beijing National Laboratory for Molecular Sciences, Key Laboratory of Polymer Chemistry & Physics of Ministry of Education, College of Chemistry & Molecular Engineering, Peking University, Beijing 100871, PR China
[b] Department of Materials Science and Engineering, University of Illinois at Urbana-Champaign, Urbana, IL 61801, USA

ARTICLE INFO

ABSTRACT

DNA complex has been widely used as non-viral vectors for the delivery of genes or siRNA. Owing to the strong and long-ranged electrostatic interaction, the structure and property of the DNA complex should evolve with time in a long-term. To test this hypothesis, we choose 2000 bp double-stranded DNA and 21 bp oligonucleotide as the model molecules, and comparatively studied their complexation with narrowly-distributed poly-L-lysine (PLL$_{150}$) by time-resolved laser light scattering. In the time range of about one week, the complexation of both DNA samples underwent three stages: formation of preliminary complex, further aggregation, followed by precipitation. The aggregation and precipitation rate of the complex formed by oligonucleotide was much faster than that of the complex formed by 2000 bp dsDNA. After precipitation, the amount of the longer chain polyelectrolyte, as determined by UV and fluorescence, was about twice that of the short chain polyelectrolyte in the sediment. The precipitates were far from being fully neutralized. Moreover, the component ratio in the sediment was independent of the mixing charge molar ratio. A rational complex mechanism was proposed on the basis of these findings. During complexation, the relaxation of polyelectrolyte inside the complex and the exchange of polyelectrolyte between complex determined the aggregation and precipitation rate. The competition of the two kinetic processes governed the structure and property of the complex in the solution and in the sediment.

1. Introduction

In the past few decades, the polyelectrolyte complexes have attracted much interest not only because of their relevance to coating, flocculation and coacervation, but also due to their application as non-viral vectors for the delivery of DNA, siRNAs and oligonucleotides [1–6]. The study on the electrostatic interactions between oppositely charged molecules may facilitate the elucidation of the mechanism of DNA packaging and gene transfection [7]. The gene therapeutics involved not only the plasmid DNA of thousands base pair long, but also short double-stranded RNAs, e.g. siRNA [8]. It has been reported that the complexation behavior of siRNA was different from that of plasmid DNA [8]. Our previous studies demonstrate that the complex formed by short oligonucleotide is in solid sphere conformation, while the complex formed by long-chain DNA is in random coil conformation with the same

condition [9,10]. Moreover, the complex formed by oligonucleotide or siRNA is not stable, which precipitates out of the solution and deteriorated the transfection efficiency [9]. But such phenomenon has never been reported on long chain DNA. So revealing the mechanism of formation of the polyelectrolyte complexes is the prerequisites for successful gene therapeutics.

The complexation of polyelectrolytes is a complicated process. Prior studies have demonstrated that a variety of parameters, such as polymer chain length and topology [11,12], charge density [13], complex charge molar ratio [14], ionic strength [15], solvent polarity [16], and order of mixing [17], have profound effect on the complexation process, the structure and the stability of the complex. It is commonly believed that the structure of the polyelectrolyte complex was controlled by kinetics [18,19]. The complex adjusted its structure via segment relaxation or displacement of molecules during the complexation process [20–22]. Cini et al. have reported that the complexes released the counterions to adjust its charge, and this process was accompanied by some progressive sedimentation [17]. Lai et al. monitored the complexation of DNA and poly-L-lysine for several hours, and found that the adjustment of the complexes was dependent on the concentration

and the mixing ratio [23]. Kuehn et al. studied the complexation of pUC19 DNA and brushed polycation by stopped flow light scattering and found that the polyelectrolyte complex was formed in the order of several tens of microseconds [24]. Even though the polyelectrolyte complex has been widely studied for more than half a century, a clear picture of the whole complexation mechanism is still missing.

Herein, we systematically studied the complexation of two DNA samples, 21 bp oligonucleotide and 2000 bp salmon testes DNA, with narrowly distributed (poly-L-lysine) (PLL$_{150}$) by a variety of physical techniques. The long-term kinetics of complexation was monitored by time-resolved laser light scattering in a non-disturbing mode. Results showed that the DNA/PLL complex was formed right after mixing, but it underwent further aggregation with time and eventually reached the thermodynamic equilibrium state: phase separation. The morphology of the complex at different time period was studied by AFM. We also determined the chemical composition of the complex after phase separation and re-examined the role of ionic strength in polyelectrolyte complexation. A rational mechanism was proposed on the basis of our findings.

2. Experimental section

2.1. Materials

Salmon testes dsDNA (~2000 bp) was purchased from Sigma Co. (USA) and used as received. The complementary 21 nt oligo-nucleotide strands: 5′-(CTTACGCTGAGTACTTCGATT)-3′ and 5′-(AATCGAAGTACTCAGCGTAAG)-3′ were purchased from Invitrogen (Shanghai, China). The sequence was designed to be structurally similar to the 21 nt siRNA which was complementary to a region of *firefly luciferase* transgenes, pGL3 [10]. The stock solution of 21 bp oligonucleotide at 2.0×10^{-3} g/mL was obtained by mixing the two complementary strands at stoichiometric ratio in $1\times$ PBS buffer, heating to 95 °C for 5 min, and annealing to room temperature. It was diluted to 5.0×10^{-5} g/mL by the buffer needed. Poly-L-lysine (PLL, average degree of polymerization is about 150) was synthesized according to a known procedure [25]. Fluorescein isothiocyanate labeled PLL (FITC-PLL, average degree of polymerization is about 150) was purchased from Sigma Co. (USA). The $1\times$ PBS buffer (pH 7.4, containing 137 mM NaCl, 2.7 mM KCl, 4.3 mM Na$_2$HPO$_4$, and 1.4 mM KH$_2$PO$_4$) was purchased from Invitrogen (Shanghai, China). The phosphate buffers (10 mM NaH$_2$PO$_4$, pH, 7.4) with different salt concentration were homemade. PLL and ~2000 bp DNA were dissolved directly by the known buffer to 5.0×10^{-5} g/mL.

2.2. Light scattering measurement (LLS)

Both static light scattering (SLS) and dynamic light scattering (DLS) experiments were conducted on a commercialized spectrometer (Brookhaven Inc., Holtsville, NY) equipped with a BI-200SM goniometer and a BI-TurboCorr digital correlator. A solid-state laser polarized at the vertical direction (GXL-III, 100 mW, CNI, Changchun, China) operating at 532 nm was used as the light source. In SLS, the angular dependence of the excess scattered intensity, $I_{ex} = I_s - I_0$ (with I_s and I_0 being the scattered intensity form solution and solvent, respectively), was measured. Since the specific refractive index increment values, dn/dC, for PLL and DNA are close, 0.16−0.17 mL/g, the I_{ex} at zero scattering angle is proportional to the molecular weight of the complex. The details can be found elsewhere [26].

All the solutions were filtered by 0.22 μm PES filters (Millipore, USA) before mixing to remove dust. The complex at varying charge molar ratio was prepared by adding PLL to DNA or vice versa. This time point was marked at t_0. The mixture was quickly vortexed at ~2000 rpm for 10 s, and the first measurement on the scattered intensity was completed in 30 s.

2.3. UV and fluorescence measurements

UV measurements were conducted on a Hitachi U-4100 instrument. The absorbance from 220 nm to 350 nm was collected. To eliminate the effect of scattering caused by the complex of large size, the absorbance at 260 nm minus that at 350 nm was used to determine the concentration of DNA in the complex [15].

Fluorescence measurements were conducted on a Horiba Jobin Yvon FluoroMax-4P instrument. The excitation and detection wavelength are 492 nm and 520 nm, respectively. FITC-PLL was used to form complex with DNA. The amount of tag in FITC-PLL was less than 1%, and its effect on the complexation was negligible. The concentration of oligonucleotide or DNA was fixed. Different amount of PLL was added into the oligonucleotide or DNA solution to form precipitate. The sample was sealed and undisturbed at r.t. for 1 month for the phase separation to complete. The top layer was transferred to a separate vial. The sediment was re-dissolved in 2 M NaCl. The concentration of the DNA was determined by the UV absorbance at 260 nm, and the concentration of FITC-PLL was determined by photoluminescence spectra.

2.4. Atomic force microscopy (AFM)

AFM measurements were conducted in tapping mode on Nanoscope III (Veeco Instrument Inc., USA) with a 110 μm scanner. The data were collected in air by a commercial silicon tip (SI-DF3, Seiko instruments Inc.). The resonant frequency of the cantilever is ~70 kHz. The complex was prepared by following the same procedure used in light scattering measurement. At each time point, 20 μL sample solution was collected at a position about 5 mm to the bottom of the vial. The sample is then deposited on a freshly cleaved mica surface. The extra solution was removed by filter paper after 30 s 20 μL Milli-Q water was then applied to rinse the surface twice. The sample was dried at room temperature for 1 day before the AFM measurement.

3. Results

DNA was a strong charged polyelectrolyte. Its charge density was twice that of PLL. The PLL with 150 repeating units was in single chain conformation at 5.0×10^{-5} g/mL in PBS buffer, and so were the 2000 bp DNA and 21 bp ds-oligo [10]. PLL and the two DNA samples were mixed, separately, at different charge molar ratios. The time dependence of the scattered intensity at 30° and the hydrodynamic radius of the complexes were monitored by laser light scattering right after mixing. Fig. 1 compares the time-dependence of the excess scattered intensity of the complexes at different +/− ratios (adding DNA into PLL) or −/+ ratios (adding PLL to DNA). In the time scale of about 1 week, only the complexes formed by adding PLL to ~2000 bp DNA (DNA in excess, Case D) showed an almost constant scattered intensity. In all the other three cases, the excess scattered intensity increased to a maximum value, and then slowly dropped to a level close to that of the solution before mixing. The UV absorbance of DNA (filled symbols in Panel A) indicated that the amount of DNA in the system started to decrease at very beginning, while the scattered intensity still increased. The combination of the excess scattered intensity and the UV absorbance data indicated that the complexation of oppositely charged polyelectrolytes was a complicated process, during which the aggregation and precipitation could coexist. The
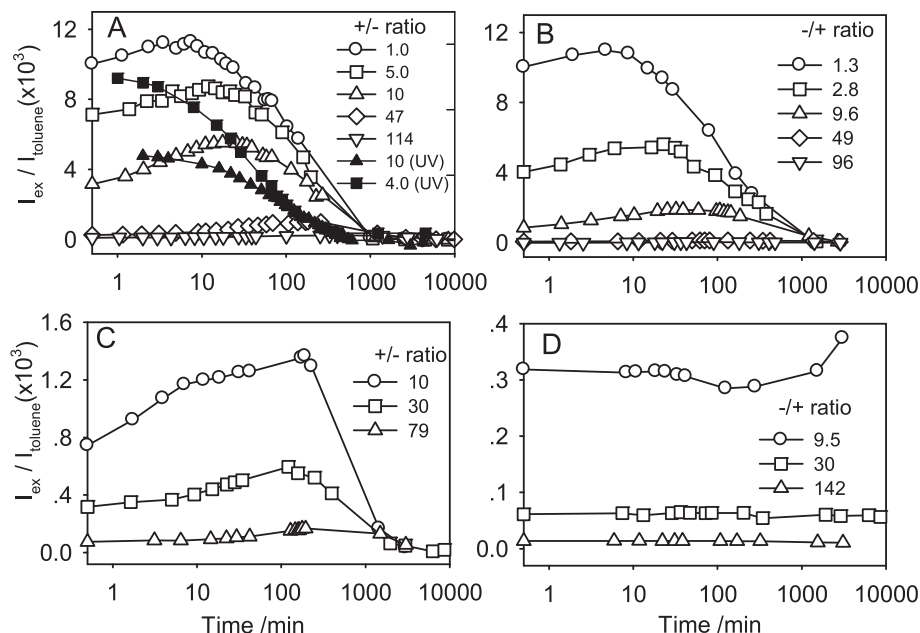
Fig. 1. Time-dependence of the excess scattered intensity at 30° for the complexes prepared by (A) adding oligonucleotide to PLL, (B) adding PLL to oligonucleotide, (C) adding salmon DNA to PLL, and (D) adding PLL to salmon DNA. The numbers in each panels were +/− molar ratio (with PLL in excess) or −/+ molar ratio (DNA was excess). The two curves with filled symbols show the changes of UV absorbance ($A_{260nm} − A_{350nm}$) with time at corresponding +/− ratios. All the samples were prepared in 1× PBS buffer (salt concentration, 150 mM), and the initial concentration of the reagents was $5.0 × 10^{-5}$ g/mL.

aggregation dominated at the beginning and was taken over by precipitation, at which point the scattered intensity reached maximum. In all the three cases (Panels A–C), the initial aggregation was heavier at the mixing charge ratios close to unity, and the precipitation was faster, too, which was demonstrated by the shorter time to reach the maximum value of the excess scattered intensity. As the intensity decreased, the fluctuation of intensity became more severe. No reliable data on size can be obtained when the fluctuations became too large. This indicated the occurrence of macrophase separation.

The complex formed by adding PLL to 2000 bp DNA (Case D in Fig. 1) seemed to be a special case. The scattered intensity (Fig. 1D) kept almost constants. No apparent aggregation or precipitation was observed in the studied time period, indicating that the complexes with 2000 bp DNA in excess were more stable than those with short chain polyelectrolyte in excess.

The first time point in Fig. 1 was 30 s after mixing. The corresponding scattered intensity, even at the charge molar ratios far from unity, was much larger than any of the individual polyelectrolyte, implying that a complex was formed immediately after mixing the oppositely charged polyelectrolytes together. The kinetic curves in Fig. 1 show that the polyelectrolyte complex underwent three stages with time: formation of preliminary complex, further aggregation, followed by or together with precipitation.

3.1. Formation of preliminary complex

Kuehn et al. had reported that the preliminary polyelectrolyte complex formed in the order of several tens of microseconds [24]. The time scale was too short for time-resolved LLS. However, the preliminary complex can be detected if it was stable with time, which was the case for the complex formed by adding PLL into 2000 bp DNA (Case D in Fig. 1). Assuming that the changes of the primary complexes in the other three cases were not prominent in the first 30 s, we can treat the firstly measured complex by LLS as the preliminary one.

Using the complex formed by adding oligonucleotide to PLL as an example, the initial scattered intensity exponentially increased as the +/− ratio reached unity, so did the average $R_{h,app}$ (Fig. 2A). Even at +/− ratio of 114, the scattered intensity was about 50 times higher than that of PLL or oligonucleotide at similar concentrations. The $R_{h,app}$ of the complex was 113 nm, which was also much larger than the size of either oligonucleotide or PLL. Therefore, the complexation at the early stage, especially in the case of oligonucleotide, should be based on the aggregation of multiple polyanions interacting with multiple polycations. Similar results were obtained in other complexes.

It was known that the addition of monovalent salts effectively screened the electrostatic interactions, which would hinder the formation of preliminary complexes. Fig. 2B–D compares the salt dependence of the preliminary complex formed by adding oligonucleotide to PLL, adding 2000 bp DNA to PLL, and adding PLL to 2000 bp DNA. The complex formed by adding PLL to oligonucleotide showed no prominent difference from the one prepared by the inverse order. Clearly, the salt-dependence of the initial excess scattered intensity showed similar trend for all the complexes: firstly increased to a maximum value at salt concentration of 270 mM, then decreased to buffer level. No complex was formed at the salt concentrations above 1 M. The salt concentration (270 mM) at which the intensity reached the maximum value was independent of the type of DNA, the order of mixing, and the size of the complex. The non-monotonic change of the scattered intensity with increasing salt concentration indicated the coexistence of long-ranged electrostatic repulsion and short-ranged attraction during polyelectrolyte complexation as suggested by Stradner et al. [27].

4. Further aggregation

Except the complex formed by adding PLL to 2000 bp DNA, all the others underwent further aggregation and precipitation with time (Fig. 1). There was no clear boundary between aggregation and
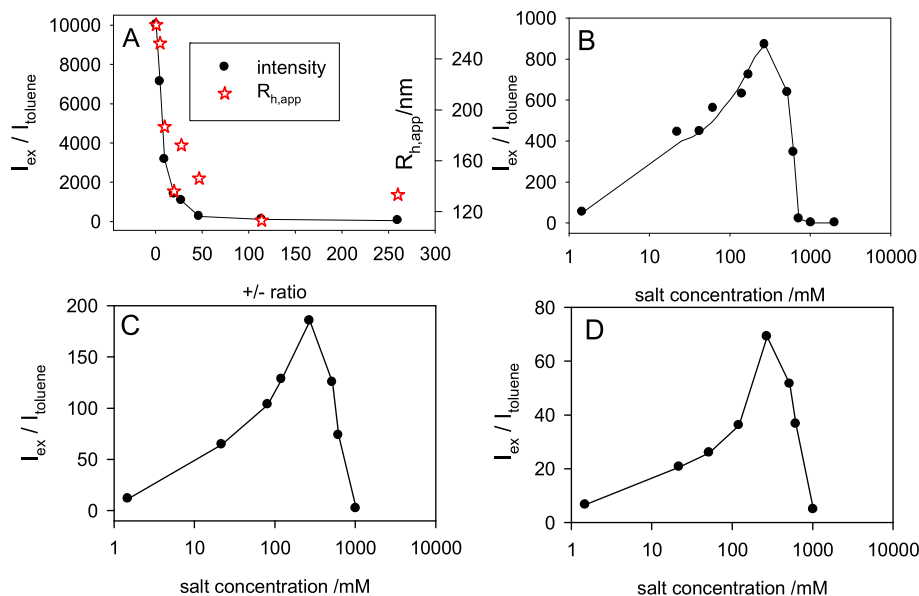
Fig. 2. Initial excess scattered intensity and $R_{h,app}$ of the complex prepared by adding oligonucleotide to PLL in 1× PBS buffer (salt concentration: 150 mM) (A). The salt dependence of the initial excess scattered intensity of the complex prepared by (B) adding oligonucleotide to PLL; (C) adding 2000 bp DNA to PLL; and (D) adding PLL to 2000 bp DNA at fixed +/− charge ratio of 30. The scattering angle was 30° and the data was collected 30 s after mixing.

precipitation. However, the scattered intensity exhibited heavy fluctuation and no reliable size can be obtained when precipitation dominated. Only the diffusive mode of the complex was detected by DLS during the aggregation process (data not shown). The excess free PLL or DNA, if there was any, made negligible contribution to the scattered intensity and cannot be detected. The size change of the complexes at different charge ratios are summarized in Fig. 3. The size increased with time in all cases, including the complex prepared by adding PLL to 2000 bp DNA, which was very slow. In general, the size was larger at the charge ratios close to unity.

Fig. 3 shows that the complex size formed by oligonucleotide was comparable to those formed by 2000 bp DNA while the former

one had a higher scattered intensity (Fig. 1) at similar charge molar ratios. According to the light scattering theory, the scattered intensity was proportional to the particle molecular weight at fixed concentration. So higher scattered intensity indicated higher molecular weight. The segmental density was defined as $\rho = 3M_{w,app}/4\pi N_A R^3$. Therefore, can be used to represent the segmental density. On the basis of the data in Figs. 1 and 3, the complexes formed by oligonucleotide possessed higher segmental density than those formed by 2000 bp DNA. Our group had reported that the complexes formed by PLL and oligonucleotide were in solid spherical conformation, while those formed by PLL and longer DNA preferred coiled conformation [10]. In general, the spherical conformation
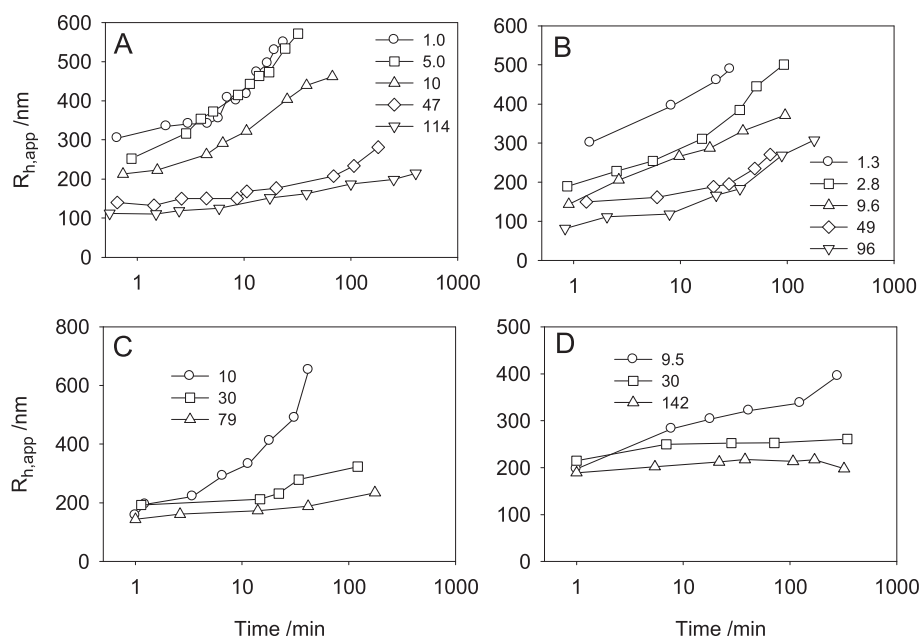

Fig. 3. Time dependence of the hydrodynamic radius of DNA/PLL complexes measured at 30° in 1× PBS buffer. (A) Adding 21 bp DNA into PLL, (B) adding PLL into oligonucleotide, (C) adding 2000 bp DNA into PLL, and (D) adding PLL into 2000 bp DNA. The numbers in the legend stand for the charge molar ratios (+/− for A and C, −/+ for B and D) of mixing.

usually had higher segmental density than coil. Higher segmental density would result in faster kinetic process. So the precipitation rate of the complex formed by oligonucleotide was faster than those formed by 2000 bp DNA.

AFM was conducted to confirm the morphology of the DNA complex prepared at different conditions. Fig. 4 shows the morphologies of the complexes at different time points. In cases A–C, large complexes were formed in the beginning (2 min). The size of the complex further increased with time. Combined with the scattered intensity (Fig. 1), the disappearance of the particles in 4.5 h indicated that most of the complexes were precipitated. Only free polymer chains or small size complex stayed in the solution. The complex formed by adding PLL to 2000 bp DNA (Fig. 4D) did not show complex of extremely large size or in large amount throughout the studied time period. All these results were in agreement with the data from light scattering (Figs. 1 and 3). It was noted that the mica surface is negatively charged, the complex with PLL in excess (+/− = 30) was larger and higher in the micrograph, especially for long chain DNA (Fig. 4A and C).

Salt concentration also exhibited profound effect on the aggregation of polyelectrolyte complexes. Fig. 5 compares the salt effect on the aggregation of three different complexes. All the conditions were the same. The effects of salt on the three complexes were almost identical. At 1.5 mM salt concentration, the complex showed weak scattered intensity and relatively smaller size, but it was stable at the studied time period. When the salt concentration was above 1 M, no complex was observed. This phenomenon of no complex formation at high ionic strength was common and it was contributed to the fully screening of the electrostatic interaction [28,29]. At intermediate salt concentration (the salt concentration in physiological condition, 150 mM, fell in this range), the time point for the scattered intensity to drop was earlier with increasing salt concentration. The earliest time point was at 520 mM salt concentration at the studied conditions, not the concentration

(270 mM) at which the scattered intensity of the preliminary complex reached the maximum value (Fig. 2). Again, it was independent of the type of DNA and the order of mixing.

5. Final precipitation

The initial DNA complex underwent further aggregation and precipitation with time. These processes must involve the redistribution of polymer chains inside the complex or between different complexes. The component ratio or charge ratio in the precipitates shed light on the complexation mechanism. By combining UV and fluorescence methods, we determined the DNA/PLL charge molar ratio in the final sediment after the phase separation was completed in $1\times$ PBS buffer. The complex was prepared by adding PLL to DNA samples. After the precipitation finished, the supernatant was transferred to another centrifuge tube with great care and the sediment was re-dissolved by 2 M NaCl solution. As shown in Fig. 6A, the quantity of the 21 bp oligonucleotide in the supernatant monotonously decreased with the mixing charge molar ratio until it reaches nearly zero at $+/- \sim 2$, while it showed opposite trend in the sediment. PLL stayed mainly in the sediment in the studied charge ratios. The sum of the fraction in supernatant and sediment, for both DNA and PLL, was nearly 100% in any mixing charge ratio, indicating that the precipitate had been fully re-dissolved.

Since the amount of DNA and PLL were known, we can calculate the charge molar ratios of the complex accumulated in the sediment. As shown in Fig. 6B, the charge molar ratio was fixed at about 2 in the case of 21 bp DNA complex, but it was only about 0.5 in the case of 2000 bp DNA complex. Since the chain length of PLL was in between that of 21 bp oligonucleotide and ~ 2000 bp DNAs, the determined $+/-$ molar ratios clearly indicated that the longer polyelectrolyte was in excess in the sediment. Moreover, the amount of longer chain polyelectrolyte was about twice that of the
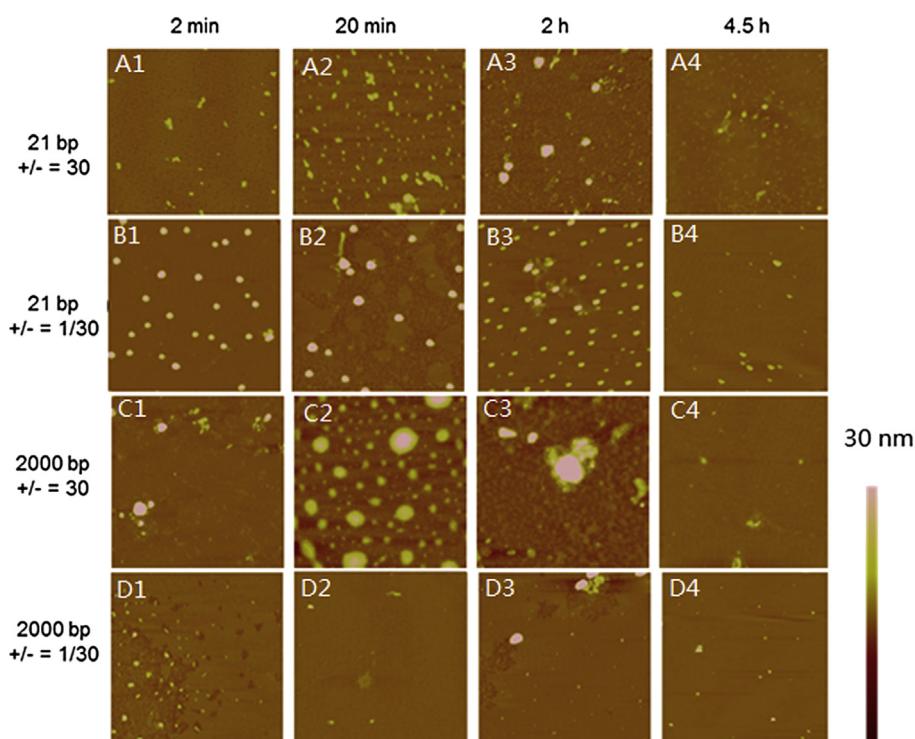

Fig. 4. AFM images of complexes in different times of complexation. Length of the side of each panel: 2 μm. Height of the scale bar: 30 nm.
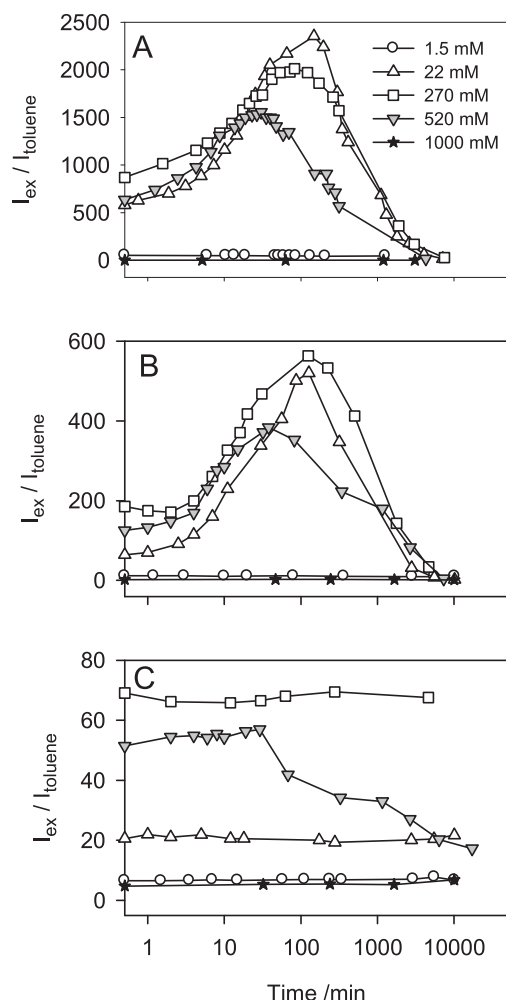
Fig. 5. Time dependence of the excess scattering intensity of the complex at different salt concentrations. The complex is prepared by (A) adding oligonucleotide to PLL; (B) adding 2000 bp DNA to PLL; and (C) adding PLL to ~2000 bp DNA. The mixing charge ratio is 30. The measurement is taken at 30°.

Fig. 6. (A) Weight fraction of oligonucleotide and PLL in both sediment and supernatant after fully precipitation in 1 month (filled symbols: sediment; hollow symbols: supernatant); (B) charge molar ratios in the sediment of the complexes. $1\times$ PBS buffer (150 mM NaCl). The standard error bar is drawn on the basis of three measurements at each point.

short chain polyelectrolyte. The precipitates were far from being fully neutralized. It has been reported that the heaviest complexation in solution (not sediment) occurred at the mixing charge ratios not exactly at one [30]. This could be explained by the unneutralized loops formed by longer chain polyelectrolyte. However, the existence of large amount of unneutralized polyelectrolyte in the sediment has not been fully realized and clarified in literature. Fig. 6B also shows that the component ratio in the sediment was independent of the mixing charge molar ratio in the studied range. This suggested that the chemical components of the precipitate were fixed once the oppositely charged polyelectrolytes were chosen.

6. Discussion

On the basis of the above results as well as those from literature, we proposed a rational mechanism of PLL interacting with oligonucleotide or 2000 bp DNA. As schematically shown in Fig. 7, the polyelectrolyte complex underwent three stages: formation of the preliminary complex right after mixing, further aggregation, and precipitation. This was independent of the mixing order. It was known that the electrostatic interaction was strong and long-ranged. On the other hand, the polycations or polyanions were
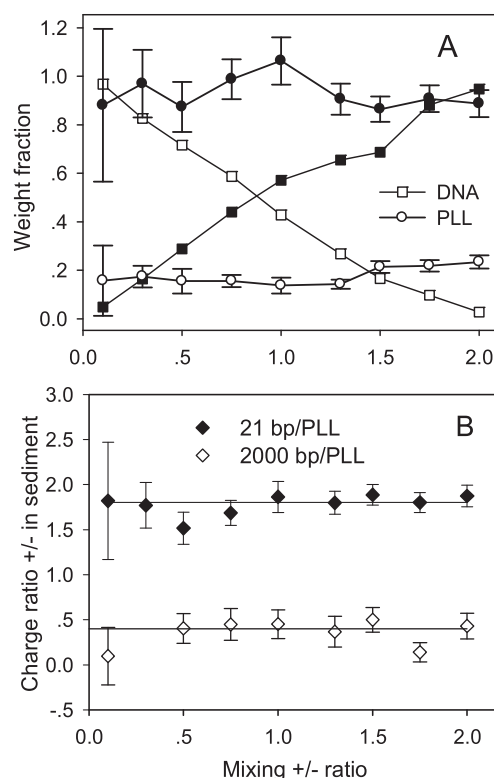
indistinguishable, and each of them had the same tendency to react with the oppositely charged polyelectrolytes surrounding it. Therefore, the preliminary complex, which was formed instantly after the mixing of the two oppositely charged polyelectrolytes, contained multiple chains. The complex based on single polycation or polyanion, which was treated widely by computer simulations, was not observed in our experiment. It could occur at extreme charge ratios or on specific polyelectrolytes [31]. Hubbe and co-workers [32] proposed "segment entrapment" model and "surface excess" model to describe the complex formed by flexible synthetic polyelectrolytes. In the "segment entrapment" model, the complex core contained unneutralized segments, while in the "surface excess" model the unneutralized segments mainly dangled on the surface. In the case of DNA and PLL, both the core and the surface of the primary complex contained charged segments or loops.

The formation of the preliminary complexes was fast, so it was not at the status favored by free energy. On one hand, the property and size of the preliminary complex were very sensitive to the preparation procedures, such as the order of mixing, the charge molar ratio, and the salt concentration, as well as the intrinsic properties of polycation and polyanion, such as the chain length. On the other hand, a large amount of charged loops formed either by polycation or polyanion existed inside the complex. Some corresponding counterions were also trapped inside the complex via counterion condensation [29,33,34]. To minimize the free energy, the polyelectrolytes, especially the one in excess, would reorganize inside the complex or among the complexes [20,35]. The segments of both polyelectrolytes thus made fine adjustment, too. All these changes would redistribute the charges of the complex, which
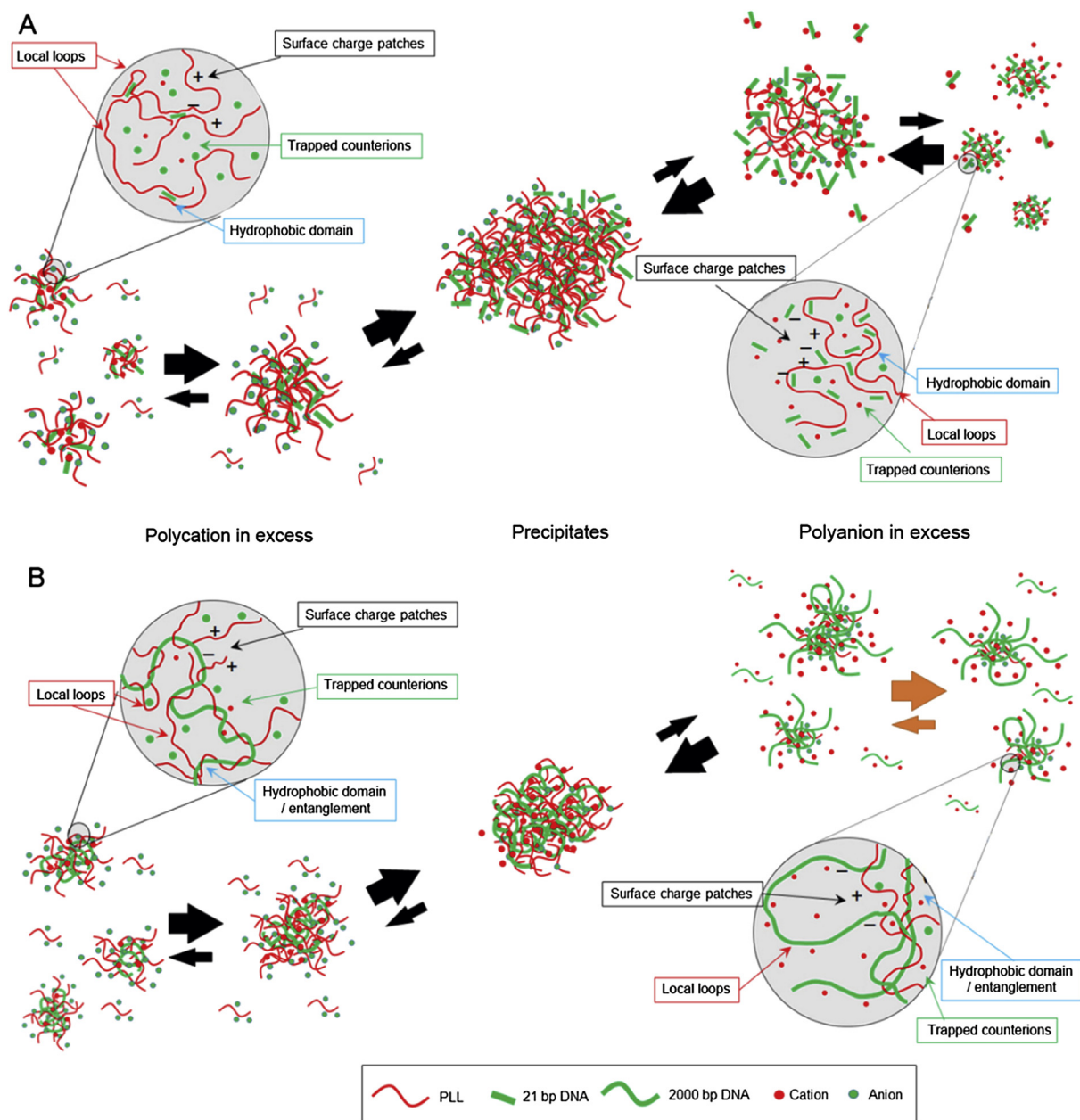
Fig. 7. Mechanism of PLL interacting with (A) oligonucleotide, and (B) 2000 bp DNA.

resulted in further aggregation or precipitation. In most cases, the precipitation of the complex (macroscopic phase separation) occurred before the completion of chain redistribution and relaxation. The precipitate contained kinetics tapped structure too. Since longer polymer chains formed more loops upon complexation, and the loops were difficult to be neutralized by chain relaxation, the charge molar ratio in the precipitate deviated from unity.

The polyelectrolyte had to overcome a barrier to allow for the redistribution and adjustment to occur. The barrier was mainly derived from the electrostatic attractions. The hydrophobic attraction and hydrogen bonding among the neutral domains were not only the driving force for further aggregation, but also the barrier for chain redistribution and segment relaxation. The relaxation was also determined by the chain conformation. It has been reported that the increase in both chain length and chain rigidity would significantly reduce the rate of chain relaxation [36–

38]. The rigidity of double stranded DNA (persistence length ∼50 nm [39]) was much larger than PLL (persistence length <2 nm [40]). Obviously, shorter polyelectrolyte chain with lower charge density had lower barriers to overcome. It was the reason for that the oligonucleotide formed a complex with higher level of aggregation, and the complex was in solid sphere conformation [10]. For the complex prepared by adding PLL to 2000 bp DNA, as schematically shown in the right panel in Fig. 7B, the inter-wound rigid-long chains were difficult to tune its structure inside the complex, or to exchange with the free chains outside the complex, due to the slow chain relaxation of the long and rigid chain [36–38]. Therefore, the complexes were trapped in a metastable state. In other words, they stayed at the stage of preliminary complex. It explained, at least partially, the findings that the complexes were easier to be kinetically stabilized by excess DNA instead of flexible polycations [15].

Depending on the charge molar ratio, the formed complex contained surface charges. The type of the charge was the same as that of the polyelectrolyte in excess [41]. Therefore, long-range electrostatic repulsion existed between different complexes, between polyelectrolytes in excess, and between complex and polyelectrolyte in excess. The short-range electrostatic attraction between the oppositely charged polyelectrolyte located mainly inside the complex. Both of the two types of electrostatic interaction were sensitive to ionic strength, but at different length scale. When the salt concentration was low, e.g. 1.5 mM, the screening of electrostatic interaction was weak, and the long-range electrostatic repulsion was strong enough to prevent the occurrence of aggregation. The complex was thus small and stable for a long time (see Fig. 5). With further increasing salt concentration, the Debye screening length decreased, and the electrostatic repulsion was deteriorated, while the short-range electrostatic attraction was basically intact. The aggregation of complex was initiated and it was getting worse as the ionic strength increased. In our system, the complexation was the heaviest at $I = 270 \pm 30$ mM, which corresponded to a Debye length of 0.6 ± 0.1 nm. Both the Bjerrum length (0.7 nm in water at 25 °C) and the spatial distance of the two adjacent charges on PLL (0.5 ± 0.2 nm, assuming the branched chains are Gaussian chain) fell in this range. This indicated that once the Debye length reached the Bjerrum length, or the distance of the adjacent charges if it was larger, further addition of NaCl did not facilitate further screening of the electrostatic repulsion, but weakened the short range electrostatic attraction, leading to a decrease in complexation. At about 520 mM, the Debye screen length reached the distance of the adjacent charges on DNA. The chain relaxation of both DNA and PLL was accelerated, resulting in a faster aggregation and phase separation rate. Above 1 M added salt, the polyelectrolyte functioned as neutral polymer, which resulted in no complex formation.

In between the complexes, there might also exist some other attraction forces, such as hydrophobic attraction [42], ion correlation attraction [43], and charge patch attraction [44]. These forces facilitated the aggregation of the complexes. But it was difficult to elucidate their specific roles by using the complexes formed by PLL and DNAs.

7. Conclusions

In summary, the complex formed by oligonucleotide and 2000 bp DNA followed similar kinetic pathway: instant formation of complex, further aggregation, followed by precipitation. However, the rate of the kinetics, as well as the morphology and composition of the formed complex were different. This was mainly caused by the fast relaxation of oligonucleotide upon forming complex. Besides the external preparation conditions, such as ionic strength and order of mixing, the design of polyelectrolyte with preferred chemical composition, architecture and topology was a practical approach to prepare complex with attractive structures trapped by kinetics. This model was also helpful for the understanding of the specific and non-specific interactions between biopolymers, such as enzyme and DNA.

References

[1] Wagner E, Cotten M, Foisner R, Birnstiel ML. Proc Natl Acad Sci U S A 1991;88(10):4255–9.
[2] Kabanov AV, Kabanov VA. Bioconjug Chem 1995;6(1):7–20.
[3] Bloomfield VA. Curr Opin Struct Biol 1996;6(3):334–41.
[4] Hu N, Johnson LM, Pothayee N, Pothayee N, Lin Y, Davis RM, et al. Polymer 2013;54(13):3188–97.
[5] Zan X, Hoagland DA, Wang T, Peng B, Su Z. Polymer 2012;53(22):5109–15.
[6] Kozhunova EY, Makhaeva EE, Khokhlov AR. Polymer 2012;53(12):2379–84.
[7] Lasic DD, Templeton NS. Adv Drug Deliv Rev 1996;20(2–3):221–66.
[8] Fattal E, Bochota A. Int J Pharm 2008;364(2):237–48.
[9] Zhou J, Liu J, Shi T, Xia Y, Luo Y, Liang D. Soft Matter 2013;9(7):2262–8.
[10] Zheng C, Niu L, Yan JJ, Liu J, Luo Y, Liang DH. Phys Chem Chem Phys 2012;14(20):7352–9.
[11] Zelikin AN, Izumrudov V. Macromol Biosci 2002;2(2):78–81.
[12] Jusufi A, Borisov O, Ballauff M. Polymer 2013;54(8):2028–35.
[13] Ren Y, Jiang XA, Pan D, Mao HQ. Biomacromolecules 2010;11(12):3432–9.
[14] Storkle D, Duschner S, Heimann N, Maskos M, Schmidt M. Macromolecules 2007;40(22):7998–8006.
[15] Izumrudov VA, Wahlund PO, Gustavsson PE, Larsson PO, Galaev IY. Langmuir 2003;19(11):4733–9.
[16] Jiang X, Qu W, Pan D, Ren Y, Williford JM, Cui HG, et al. Adv Mater 2013;25(2): 227–32.
[17] Cini N, Tulun T, Blanck C, Toniazzo V, Ruch D, Decher G, et al. Phys Chem Chem Phys 2012;14(9):3048–56.
[18] Sunoqrot S, Liu Y, Kim DH, Hong S. Mol Pharmacol 2013;10(6):2157–66.
[19] Lindhoud S, Norde W, Stuart MAC. J Phys Chem B 2009;113(16):5431–9.
[20] Li Y, Bronich TK, Chelushkin PS, Kabanov AV. Macromolecules 2008;41(15): 5863–8.
[21] Dias RS, Linse P, Paisi AACC. J Comput Chem 2011;32(12):2697–707.
[22] Raspaud E, Pitard B, Durand D, Aguerre-Chariol O, Pelta J, Byk G, et al. J Phys Chem B 2001;105(22):5291–7.
[23] Lai E, van Zanten JH. Biophys J 2001;80(2):864–73.
[24] Kuehn F, Fischer K, Schmidt M. Macromol Rapid Commun 2009;30(17):1470–6.
[25] Lu H, Cheng JJ. J Am Chem Soc 2007;129(46):14114–5.
[26] Zhou JH, Ke FY, Xia YQ, Sun JB, Xu N, Li ZC, et al. Polymer 2013;54(10):2521–7.
[27] Stradner A, Sedgwick H, Cardinaux F, Poon WCK, Egelhaaf SU, Schurtenberger P. Nature 2004;432(7016):492–5.
[28] Sukhishvili SA, Kharlampieva E, Izumrudov V. Macromolecules 2006;39(26): 8873–81.
[29] Dobrynin AV, Rubinstein M. Prog Polym Sci 2005;30(11):1049–118.
[30] Raspaud E, Pelta J, de Frutos M, Livolant F. Phys Rev Lett 2006;97(6). 068103-068101-068104.
[31] Dai ZJ, Wu C. Macromolecules 2012;45(10):4346–53.
[32] Chen J, Heitmann JA, Hubbe MA. Colloids Surfaces Physicochem Eng Aspects 2003;223(1–3):215–30.
[33] Manning GS. J Chem Phys 1969;51(3):924–33.
[34] Heyda J, Dzubiella J. Soft Matter 2012;8(36):9338–44.
[35] Kizilay E, Kayitmazer AB, Dubin PL. Adv Colloid Interface Sci 2011;167(1–2): 24–37.
[36] van der Zande BMI, Dhont JKG, Bohmer MR, Philipse AP. Langmuir 2000;16(2):459–64.
[37] Kumar A, Biswas P. J Chem Phys 2011;134(21):214901–10.
[38] Sato T, Ohshima A, Teramoto A. Macromolecules 1994;27(6):1477–83.
[39] Hays JB, Magar ME, Zimm BH. Biopolymers 1969;8(4):531–6.
[40] Davidson B, Fasman GD. Biochemistry (Mosc) 1967;6(6):1616–29.
[41] Raspaud E, Chaperon I, Leforestier A, Livolant F. Biophys J 1999;77(3):1547–55.
[42] Ha JH, Spolar RS, Record MT. J Mol Biol 1989;209(4):801–16.
[43] Rouzina I, Bloomfield VA. J Phys Chem 1996;100(23):9977–89.
[44] Sennato S, Bordi F, Cametti C, Diociaiuti M, Malaspina P. Biochim Biophys Acta Biomembr 2005;1714(1):11–24.